3D Large Deformation Finite Element Analyses of Jack-up Reinstallations Near Idealised Footprints

Wensong Zhang, Mark J. Cassidy and Yinghui Tian

Centre for Offshore Foundation Systems and ARC CoE for Geotechnical Science and Engineering,

THE UNIVERSITY OF WESTERN AUSTRALIA

ABSTRACT

The potential risks that are present during a reinstallation process of a jack-up located alongside existing footprints that were left on a seabed during previous operations are an important concern. Uneven soil surface and strength heterogeneity within the footprint can cause large eccentric and inclined loading conditions, potentially exceeding the structural capacities of the jack-up or producing dangerous movement towards a production platform. Advice on safe installation procedures is extremely limited in the literature. Although a range of experimental modelling has been carried out to address this problem, a robust and accurate numerical framework is yet to be developed to improve the understanding of the jack-up reinstallation processes.

In this study, spudcan reinstallation processes near idealised footprints were successfully simulated using the recently developed 3D large deformation finite element (LDFE) method. Large variations in the footing load conditions were observed with significant transitions in the soil deformation mechanism. The quantitative predictions of vertical (V), horizontal (H) and moment (M) loads exerted on the spudcan matched closely with previous centrifuge data. The critical spudcan reinstallation offset distances at which the maximum horizontal and vertical loads are most likely to occur are found to be between a half and one footing diameter way from the centre of the footprint. Potential applications of this 3D LDFE method in parametric and full-scale case studies are summarised at the end of this paper.

KEY WORDS: 3D LDFE, 3D RITSS, Jack-up reinstallation, Jack-up footprints, offshore engineering

INTRODUCTION

Jack-up units have been commonly used for drilling in oil and gas fields in shallow to moderate water depths. These units typically consist of a floating hull structure and three retractable truss-work legs with large, inverted, conical-shaped foundations called ‘spudcans’. Seabed depressions, which are known as ‘footprints’, are often created during the removal of jack-up units as the spudcans retract.

Nowadays, jack-up platforms may need to be re-installed near existing footprints for various purposes, such as additional drilling or servicing a fixed platform (Figure 1a). The presence of footprints complicates the reinstallation processes by introducing inclined and eccentric loads onto the spudcans and leg structures, which in turn can cause excessive lateral and rotational displacements. However, limited design guidelines are available for geotechnical engineers to manage these situations. In SNAME (2008)[1], a reinstallation distance of at least one spudcan diameter from the edge of the footprint is recommended. For the cases where overlap with the footprint is inevitable, jack-up units with identical spudcan geometry and leg spacing are advised for use, with one of the spudcans positioned at the centre of the previous footprint to minimise any non-vertical load that could cause severe damage to the platform. However, this procedure is impractical in many situations.

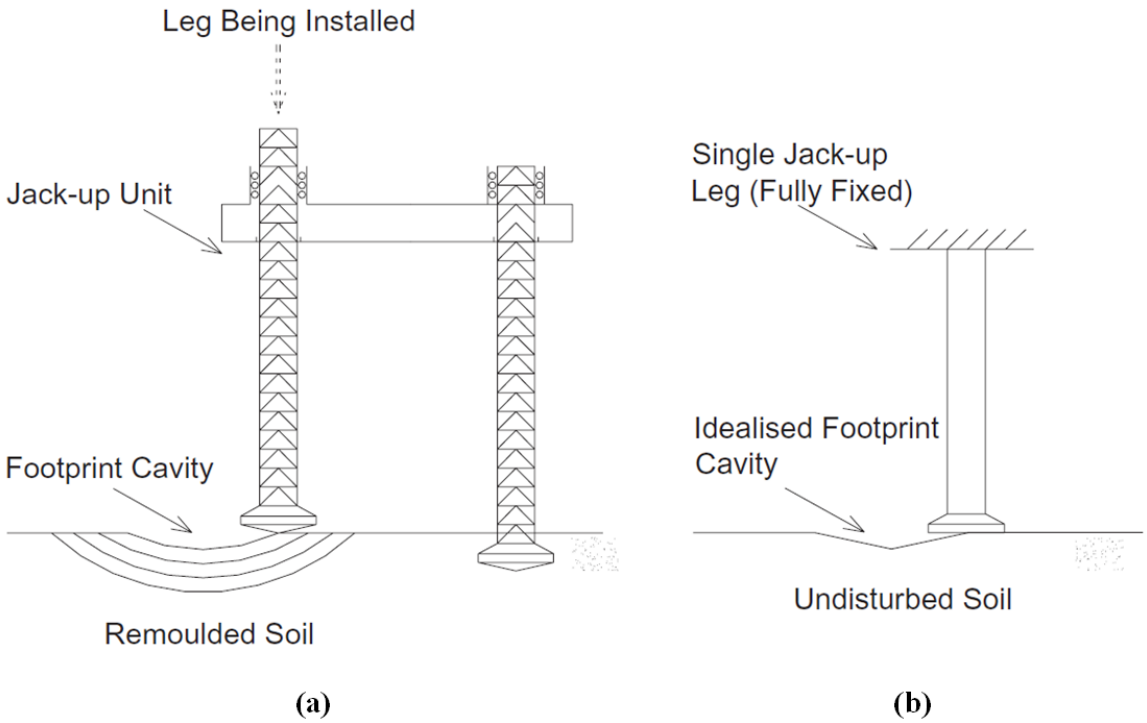

Figure 1. Reinstallation processes of jack-up units under (a) a real situation and (b) an idealised situation (i.e., the situation investigated in this study) [2]

It is therefore important to investigate the influence of the previous footprints on the jack-up reinstallation processes. Due to the high complexity of the problem, the majority of previous studies have been conducted using physical models within geotechnical centrifuge facilities [3-5], and the vertical (V), horizontal (H) and moment (M) loads measured to quantify the influence level. A series of parametric studies have been performed experimentally to investigate the effect of soil heterogeneity [6, 7], footprint geometry [8, 9] and leg flexibility [8, 10, 11]. Various mitigation strategies have also been proposed and then examined experimentally [12-15]. However, numerical studies on such problems remain limited primarily due to (1) the requirement of 3D large deformation simulation methods, most of which are complex and often computationally challenging, and (2) the involvement of complex soil free surfaces, which can be difficult to track and retain during simulations. Among the published numerical studies, the plane-strain assumption has been commonly adopted to simplify the simulations into 2D [13, 14], which essentially replaces circular spudcans and footprints with strip footings and infinitely long, sloped trenches. As one of the only two studies (that the authors are aware of) that managed to consider the 3D effects of the reinstallation problems, Mao et al. [16] examined the effect of the footing-footprint offset distance using the 3D Arbitrary Lagrangian Eulerian (ALE) method. However, those simulations were conducted with relatively coarse meshes and uncommon footprint geometries. Conversely, Hartono et al. [17] investigated the effect of the 'reaming' process as a mitigation strategy to the problem, in which the 3D Coupled Eulerian-Lagrangian (CEL) method was used to simulate the footprint creation and reinstallation processes. However, with only one simulation result presented, the reliability of this approach cannot be verified when considering the high numerical uncertainties in CEL simulations, as discussed by Wang et al. [18]. More accurate and comprehensive numerical studies are therefore required to provide geotechnical engineers with greater confidence when addressing jack-up reinstallation problems. This requires the development of a 3D large deformation numerical simulation solution that is capable of addressing continuous penetration problems with complex free-surface features while maintaining high simulation accuracy.

In this study, the recently developed three-dimensional large deformation finite element method (3D LDFE) is introduced and applied to numerically simulate the reinstallation processes of jack-up platforms near idealised footprints. The effect of the initial footing-footprint offset distance is investigated using this new LDFE method. The results are compared against previous centrifuge data for validation purposes, and the predicted displacement vector fields are plotted and compared against previous observational experimental results (known as the PIV method, see White et al. (2003)[19]) to identify the transitions in soil failure

mechanisms during penetration processes. A parametric study is then performed to identify the critical offset distances that lead to the maximum horizontal and moment loads on the spudcan and leg structure. This study aims to demonstrate the capability and potential of the new LDFE method in addressing complicated geotechnical problems, some of which are presented in terms of potential research topics in the conclusion of this paper.

3D RITSS METHOD

As a branch of the ALE large deformation finite element method, the 'remeshing and interpolation technique with small strain' (RITSS) approach has been widely used in both quantitative and qualitative numerical simulations to address various geotechnical problems because of its (1) high compatibility with most finite element packages, (2) high accuracy due to the use of implicit solution seeking algorithm, and (3) ability to model effective stress problems. This method was originally proposed by Hu and Randolph [20] and implemented through the use of AFENA [21] and in-house-developed mesh regeneration and field variable mapping codes. A wide range of 2D simulations have been conducted with RITSS method by taking advantage of plane strain and axisymmetric features of the originally 3D problems. Over the past ten years, a few attempts have been made to extend this method into three-dimensional problems [22, 23]; however, limited by the difficulties in high-quality 3D mesh regeneration, the implementation of the 3D RITSS method remains challenging.

A practical and robust approach to implement the RITSS method in three-dimensional problems was recently developed at the Centre for Offshore Foundation Systems (COFS), University of Western Australia (UWA) by the authors. Similar to the traditional 2D RITSS approach, the simulation consists of the following core procedures: (1) initial finite element (FE) model creation and simulation setup; (2) standard Lagrangian small-strain finite element increment; (3) deformed mesh extraction and regeneration; (4) new simulation setup with the regenerated mesh; and (5) field-variable (e.g., stress, strain) mapping from the deformed mesh to the regenerated mesh. Procedures (2) to (5) are repeated until a specific load or displacement target is met. The load or displacement enforced in each Lagrangian increment is required to be sufficiently small to avoid any severe element distortions. Among the five core procedures of the RITSS method, the realisations of procedures (3) and (5) are critical because they essentially determine the robustness and accuracy of the complete simulation. In previous RITSS applications, intensive user-defined coding has often been required to enforce these two procedures. This significantly limits the accessibility of the RITSS method and therefore makes it only available to highly experienced FE developers. Due to the complications imposed by 3D mesh regeneration, significant geometric idealisations have been applied in previous 3D RITSS applications to avoid tracking complex free surface geometries, which significantly affects the simulation accuracy.

The recently developed 3D RITSS method utilises third-party mesh regeneration software HyperMesh [24] to perform the required 3D mesh regenerations followed by element optimisations to ensure consistent meshes across increments. The mesh regeneration process executed by HyperMesh can precisely track and retain any free surfaces from the deformed mesh, which preserves important geometric features and thus increases simulation accuracy. The 'tetra mesh optimisation' feature [25] allows users to specify certain element quality criteria, such as 'aspect ratio' and 'volumetric skewness', to ensure that the regenerated meshes are of consistent quality, which helps to reduce the magnitude of numerical fluctuations in the results. Regarding the field-variable transfer processes, the new 3D RITSS method used ABAQUS's 'mesh-to-mesh solution mapping' (MSM) feature [26], which is a fully automated process that requires no user-defined coding (see Tian et al. (2014)[27] for implementation details and examples). Lagrangian small-strain finite-element increments were also performed in ABAQUS. A script written in Python, which is a mainstream programing language, is used to control the entire simulation. A more detailed description of this method will be presented in another paper later this year together with several validation examples. The distinct advantages of this new 3D RITSS method can be summarised as follows:

(1) being capable of dealing with three-dimensional problems that involve complex free surface geometries;
(2) highly consistent mesh qualities that minimise fluctuations in the result curves; and
(3) no user-defined coding required except for a single Python script for executing the simulation, thus minimising the learning and programing effort required by the user.

With regard to the computational cost for the 3D RITSS simulations, approximately 3 hours of computing time is required on a desktop computer with a 3.4 GHz CPU and 16 GB of RAM to perform a 200-increment surface footing penetration simulation with approximately 35000 first order tetrahedral elements.

ANALYSES SETUP

To provide direct benchmarking with previous centrifuge experiments, the numerical models adopted in this study closely follow the tests performed by Kong [8]. An idealised conical-shaped seabed depression with a diameter and depth of 30 m and 5 m, respectively (Figure 1b and 2) was used in this study to represent the footprint. Additionally, a flat base, circular footing is adopted instead of real spudcan models to eliminate any effects of the spudcan geometry. The footing has a diameter of D=15 m and a thickness of 1.725 m. A solid cylinder with a diameter of 6.075 m is attached to the footing to represent the leg. Because only the effect of the geometry is considered in this study, the penetration depth is limited to 0.5D to maximise the simulation efficiency. Based on Kong et al. (2010)[2], the influence of the footprint geometry on the footing reinstallation process becomes negligible after this depth for this specific footprint model. Five offset distances between β=0.55D and β=1.55D are chosen to be investigated in this study, where β is defined as the centre-centre distance between the footing and the footprint.

As illustrated in Figure 2, half models are used in these simulations to minimise the computational costs incurred. The soil domain is constructed with dimensions of 80 m×60 m×40 m. Tresca model is used to represent the Kaolin clay used in the centrifuge tests. The soil's undrained shear strength profile (s_u) is described by the following expressions:

$$s_u = \begin{cases} 7.5 + 0.92z & z < 3.4\,\text{m} \\ 5.0 + 1.68z & z \geq 3.4\,\text{m} \end{cases} (\text{kPa}) \quad (1)$$

where z is the vertical distance measured into the ground from the initial mud-line level of the undisturbed part of the soil.

To focus purely on the effect of the footprint geometry, no adjustment in the soil strength profile is made to the soil near the footprint. However, with the experimental approach, disturbance in the soil strength is inevitable when creating the footprint (Figure 3). This marginal difference in the soil profile is unlikely to cause significant differences in the results because the effect of footprint geometry should remain dominant in cases of shallow penetration on relatively stiff clays [7, 8]. A typical Young's modulus profile of $E=500s_u$ is used with a Poisson's ratio of 0.49 to account for the undrained condition. No strain softening or rate effect is considered in this study to avoid further complications. The effect of soil weight is considered by adopting a submerged unit weight of 6.82 kN/m^3.

Similar to the experimental setup, the footing is assumed to be rigid with no horizontal or rotational movements allowed (Figure 1b). As shown in Figure 2, any load being applied to or experienced by the footing will be enforced or measured at the load reference point (LRP) with the stated sign convention. The footing base is assumed to be fully 'bonded' to the surrounding soil, and the side faces are configured to have frictionless interactions with any soil elements with which they come into contact. First-order tetrahedron hybrid elements (C3D4H) are used to mesh the model. The hybrid formulation is used to mitigate any potential volumetric locking problems; additional technical details on this can be found in the ABAQUS 6.12 Theory Manual [26]. A minimum element size of 0.02D is used to minimise the numerical errors while keeping the simulations at an acceptable size.

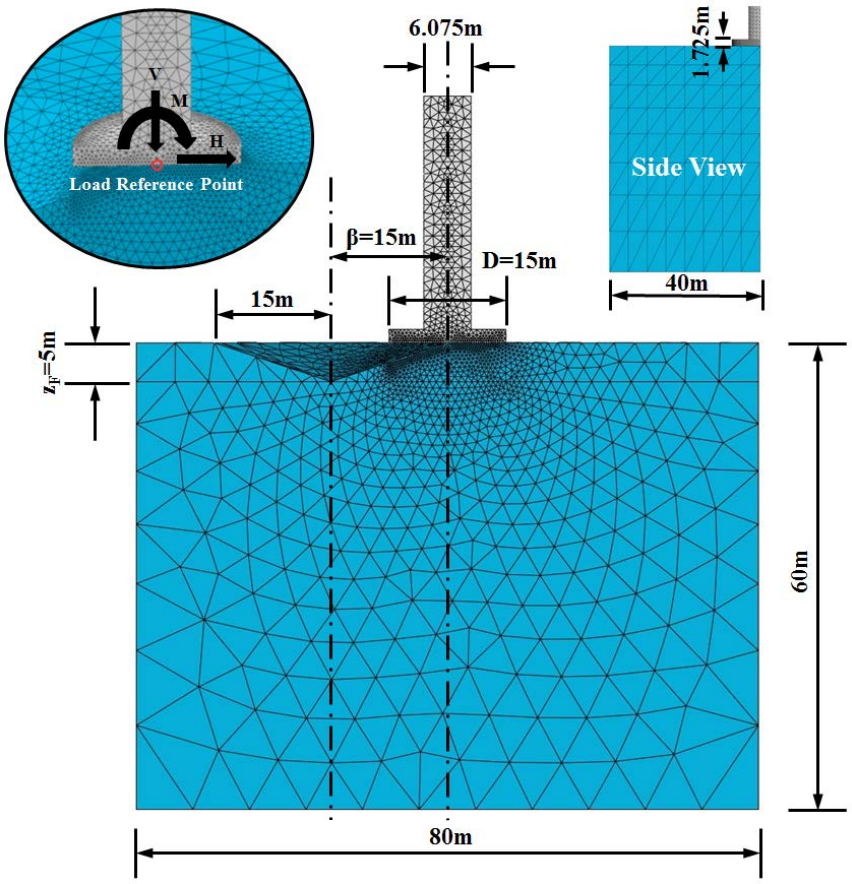

Figure 2. Sign conventions and simulation setup (β=1.0D)

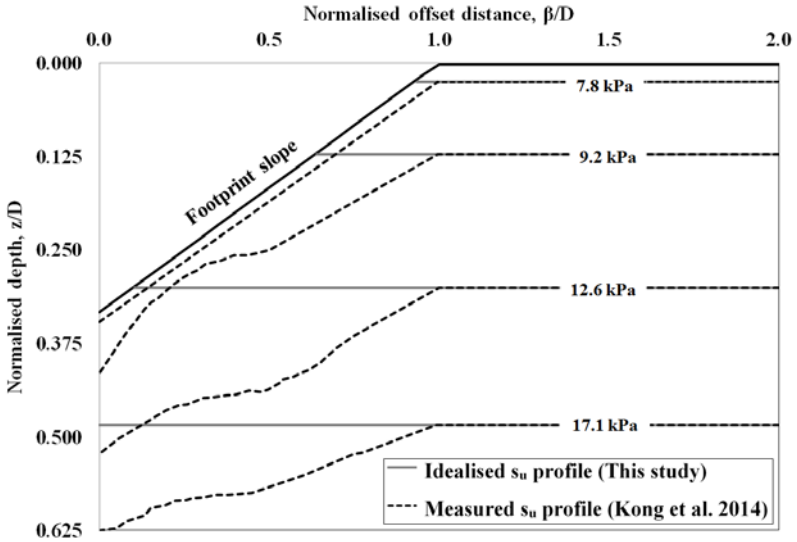

Figure 3. Difference in soil strength profiles between the experimental tests and this study

RESULTS AND DISCUSSIONS

Validation using centrifuge measurements

The VHM plots for the β=0.55D case are presented in Figure 4, and centrifuge data from tests conducted by Kong [8] with similar footprint geometry and offset distance are used as a benchmark. Positive horizontal (H) and moment (M) loads were successfully captured by the current study with a reasonable level of agreement

with the centrifuge data. As anticipated, marginally higher magnitudes were predicted in all three load components due to (1) ignoring the strain softening and rate effects and (2) the idealisation in soil strength profiles. However, similar features in the H and M plots were evident: both the horizontal and moment loads increased rapidly from the initial state; and the peak horizontal load occurred at the footprint toe level (z=0.33D) in both approaches, whereas the largest moments were predicted at a much smaller penetration depth. Both H and M reduced to an insignificant magnitude after passing the footprint toe level.

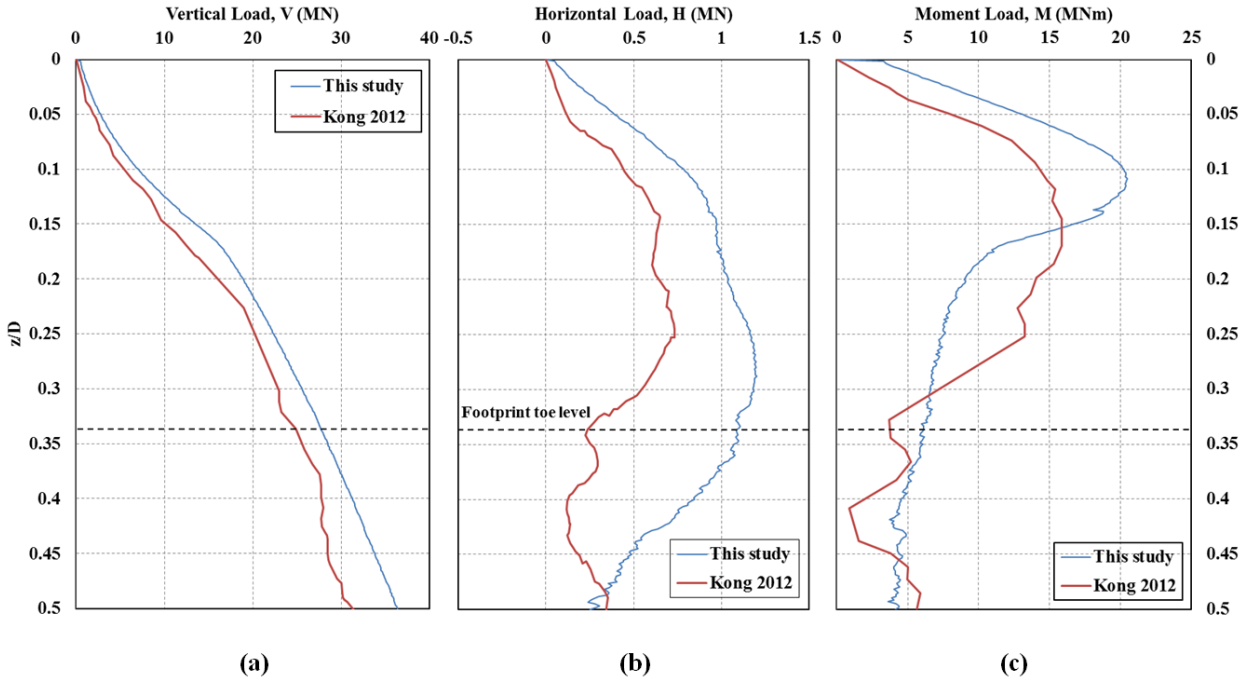

Figure 4. Comparison of the variations in the (a) vertical, (b) horizontal and (c) moment loads for the β=0.55D case predicted in this study and in the centrifuge data

To provide a more direct comparison between the numerical and physical modelling results, the horizontal and moment loads were normalised to create the load inclination (α) and eccentricity (e/D) using expressions (2) and (3). This allows the investigation of the combined load effect without the influence from the differences in the soil strength and strain effect:

$$\alpha = \tan^{-1}\left(\frac{H}{V}\right) \tag{2}$$

$$\frac{e}{D} = \frac{M}{VD} \tag{3}$$

The normalised parameters are plotted in Figure 5. Considering the level of data noise and uncertainties present in the centrifuge tests, excellent agreement was found between the two sets of data. This verifies the accuracy of the numerical method in predicting the effect of the geometry of the existing footprints on the spudcan reinstallation processes.

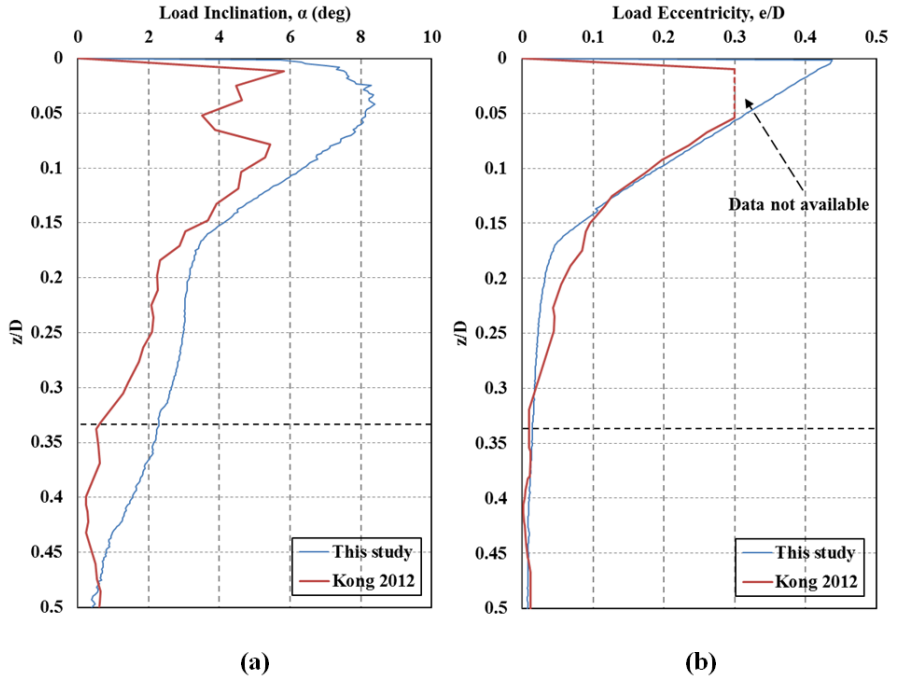

Figure 5. Variations in the (a) load inclination and (b) load eccentricity during the reinstallation process of the β=0.55D case

Soil failure mechanisms

The displacement vector fields of the β=1.0D case at various depths are presented in the right half of Figure 6. Four penetration depths are of the most interest to study the effect of the footprint geometry: the initial touchdown depth (z/D=0.05), the soil-footing full-contact depth (z/D=0.10), the footprint toe level (z/D=0.33) and the end of the influential zone (z/D=0.50). At the initial touchdown depth, an eccentric two-way failure mechanism was observed underneath the footing, where the left hand side (LHS) pushed the soil block towards the centre of the footprint. As penetration continued, the LHS shear band grew and propagated towards the toe of the footprint with a decreasing vertical load eccentricity. After the footing base came into full contact with the soil, the LHS shear band was observed passing the footprint toe. The geometry of the footprint was therefore significantly influenced by the penetration process. When the footing toe level was reached, localised soil backflow has already formed on the right hand side (RHS) of the footing, though the surface shear band could still be observed on the LHS. As the penetration depth increased further and reached a z/D value of 0.5, the localised backflow on the LHS finally started to initiate while the soil on the RHS began to collapse back onto the footing due to (1) gravity-induced slope instability and (2) the soil backflow mechanism. After passing this depth, soil began to flow back on both sides of the footing; the influence on the failure mechanism caused by the presence of the footprint geometry therefore began to fade away.

The particle image velocimetry (PIV) method has been previously used in conjunction with centrifuge tests to investigate the transition in the soil failure mechanism during reinstallation processes. In the PIV test conducted by Kong et al. [28], a flat base footing was installed near an idealised footprint with an offset distance of β=1.0D, the results of which are also presented in the left half of Figure 6. The footprint model used in the PIV test was a V-shaped, sloped footprint with the same depth and width of the footprint used in this study. Because the conical-shaped footprint model used in the numerical simulations of this study gives a larger initial contact area compared with the sloped footprint used in PIV tests, the full soil-footing contact engagement has been predicted at relatively shallower depths. However, in terms of the types and transition order of the soil failure mechanisms, strong agreements are shown between the approaches, despite their different footprint geometries.

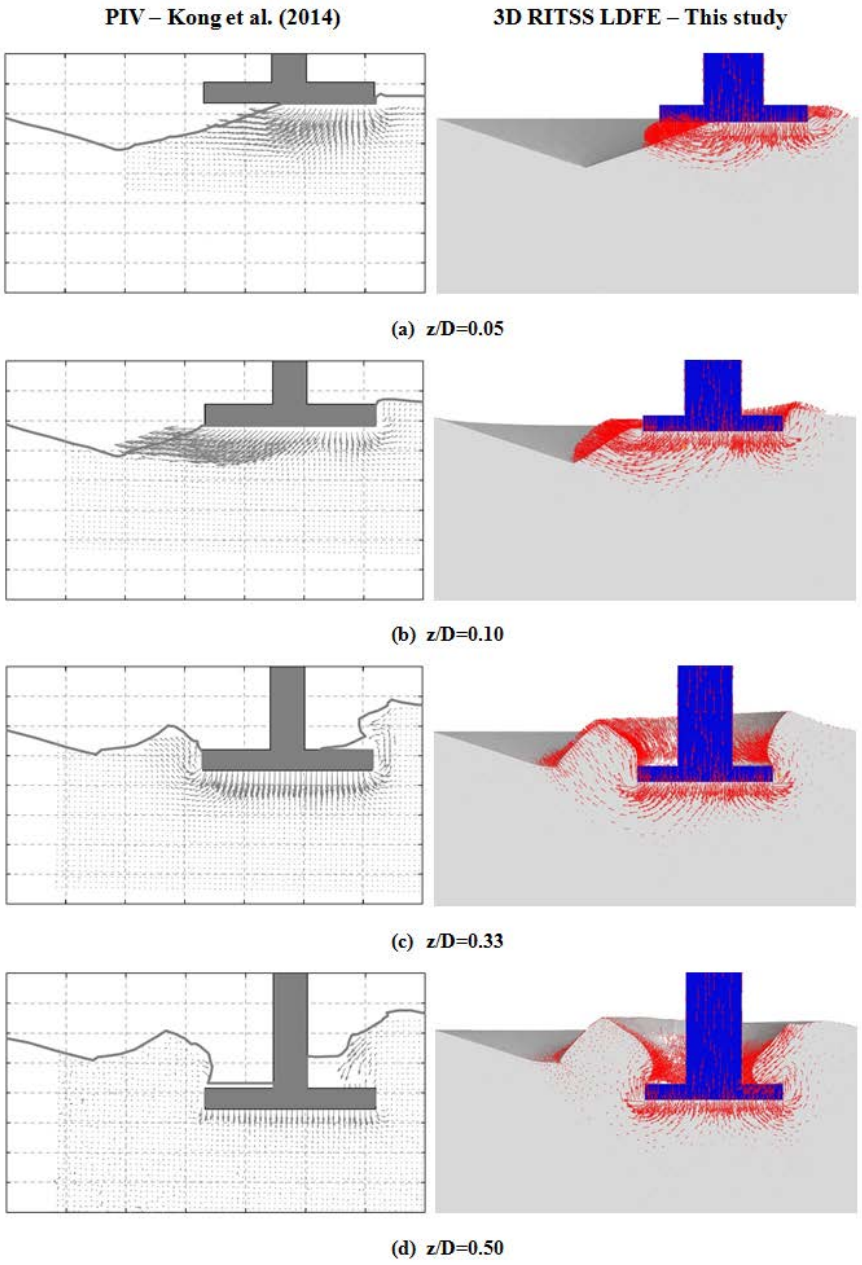

Figure 6. Comparison of soil failure mechanisms for the β=1.0D case between previous PIV test results (left) and those of this study (right)

Parametric study on offset distance

Flat base footing reinstallation processes near the idealised footprint are now simulated with five offset distances (e.g., β=0.55D, 0.75D, 1.00D, 1.25D and 1.55D). This parametric study aims to investigate the effect of offset distance on the footing load condition during reinstallation processes. The results of this analysis are plotted and presented in Figure 7. Significant deviations in the vertical penetration resistances are shown in the initial penetration stage. As expected, the magnitude of the vertical resistance increases with the offset distance as a result of increasing initial contact area. For all cases, as the penetration continues, the contact area increases rapidly and thus leads to the significant increase in the vertical resistances. The effect of footprint geometry becomes less influential on the vertical penetration resistance as the penetration depth increases, which results in the joining of the five V curves at roughly z/D=0.5.

As the two critical load components of this study, the variations in the horizontal and moment loads and their corresponding normalised parameters can be described with three key penetration stages: (1) $z<z_{contact}$; (2) $z_{contact}<z<z_F$; and (3) $z>z_F$, where $z_{contact}$ is the depth at which the soil and footing base first engages full contact, and z_F is the depth of the footprint. Stage (1) is defined as the initial penetration stage in which no

full soil-footing contact has been engaged. As shown in Figures 6 (a)-(b), the LHS shear band continues to expand throughout stage (1), which significantly increases the asymmetry of the soil block movement. Additional soil material continues to be pushed horizontally towards the centre of the footprint, thus continuously increasing the horizontal resistance. Due to the significant load eccentricity caused by the partial soil-footing contact, a large variation in the moment load is also observed within this stage. The depths at which the peak moments occur increase with decreasing offset distance. The exact magnitude of the peak moment load and its corresponding penetration depth are functions of (a) load eccentricity, which reduces with increasing penetration, and (b) vertical resistance, which increases with penetration as a result of increasing soil strength and soil-footing contact area. The load eccentricity is found to decrease linearly with the penetration depth until the full soil-footing contact depth ($z_{contact}$) is reached. At the end of this stage, the moment loads are reduced to approximately 50% of their corresponding peak values as a result of the significant reduction in the load eccentricity.

During the second penetration stage ($z_{contact}<z<z_F$), the soil heave on the RHS starts to accumulate and exerts noticeable horizontal earth pressure on the footing. The difference in the lateral earth pressure between the two sides of the footing serves as an additional component to the resultant horizontal load, which in turns leads to a further increase in the horizontal load and eventually causes the curves to reach their peak at approximately the footprint toe level. Regarding the moment loads, due to the adoption of an idealised soil profile, no significant variation in the soil shear strength is created across the footing base, and therefore, both the moment and load eccentricity continue to decrease to an insignificant magnitude.

As the footing penetrates past the footprint toe level ($z>z_F$), localised soil backflow is initiated on the LHS of the footing, which significantly reduces the asymmetry of the soil failure mechanism. As the other major source of the horizontal load, the lateral earth pressure difference also decreases due to the increasing soil height on the LHS. As a consequence, the horizontal force experienced by the footing reduces dramatically after penetrating through the footprint toe level, which also marks the end of the footprint geometric influence zone.

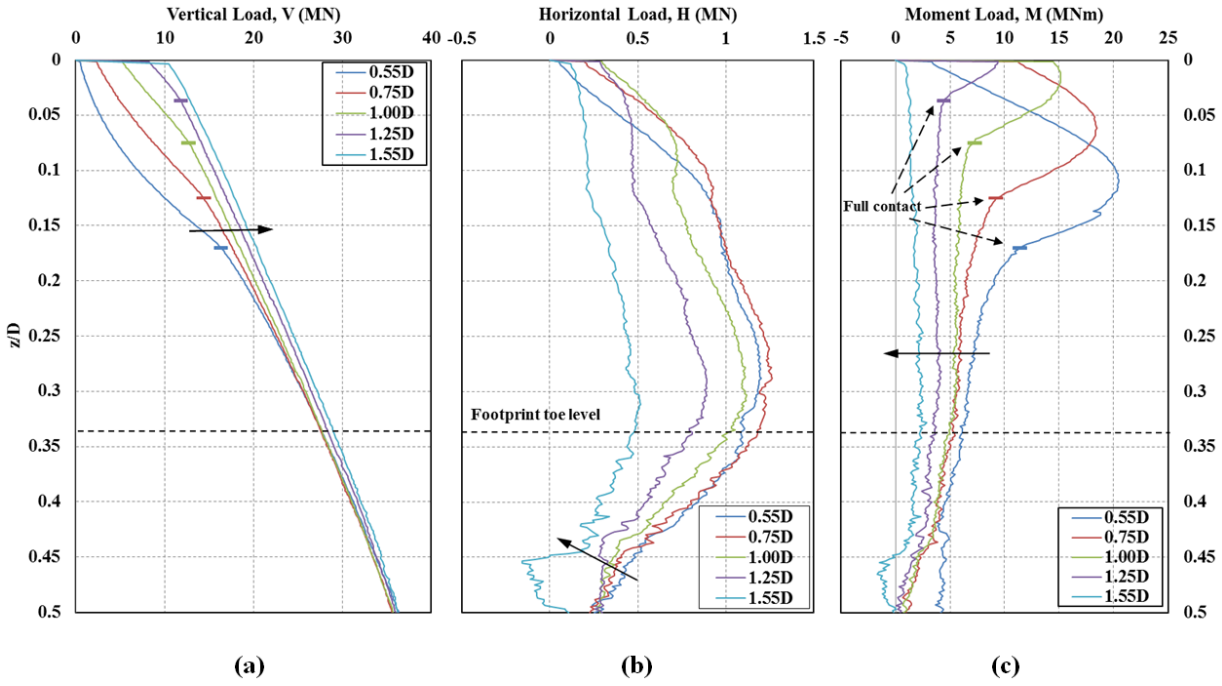

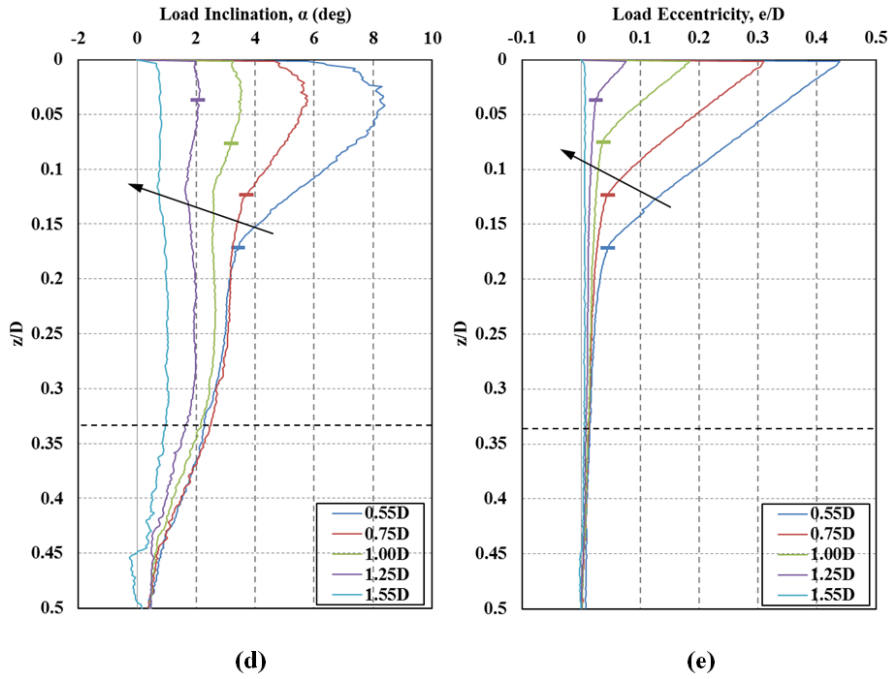

Figure 7. Offset distance (β) effect on the footing load condition during reinstallation processes

The maximum horizontal and moment loads for each offset distance are presented in Table 1 and Figure 8. Peak H_{max} and M_{max} are observed at an offset value of 0.75D and 0.55D, respectively; these findings confirm the physical modelling results of previous publications, such as references [4, 7], in which a critical offset distance range of 0.5D to 1.0D was suggested. The magnitudes of the predicted maximum loads are found to be greater than the measured values reported by Kong et al. [9]. This is due to the inevitable disturbance in the soil strength profile when creating the experimental footprints, which weakens the surrounding soil. As the offset distance increases, the influence from this weakening of the soil strength decreases. Therefore, an improved level of agreement is observed at higher offset values. The two plots shown in Figure 8 can serve as guidelines for the preliminary estimations of the extreme load conditions during jack-up platform reinstallations if the following requirements are met: (1) the jack-up legs must have high lateral and rotational structural stiffness (i.e., the lateral and rotational motions are negligible); and (2) the shallow penetration stage is of particular interest (i.e., the footprint geometry effect is dominant).

Table 1. Details of the peak horizontal and moment loads

Offset Distance (β/D)	H_{max} (MN)	z_{Hmax}/D	M_{max} (MNm)	Z_{Mmax}/D
0.55	1.20	0.288	20.48	0.108
0.75	1.26	0.288	18.45	0.062
1.00	1.12	0.303	15.17	0.017
1.25	0.89	0.304	9.41	0.002
1.55	0.52	*	2.86	*

*No obvious peak is observed at β/D=1.55; z_{Hmax} and z_{Mmax} are therefore not presented.

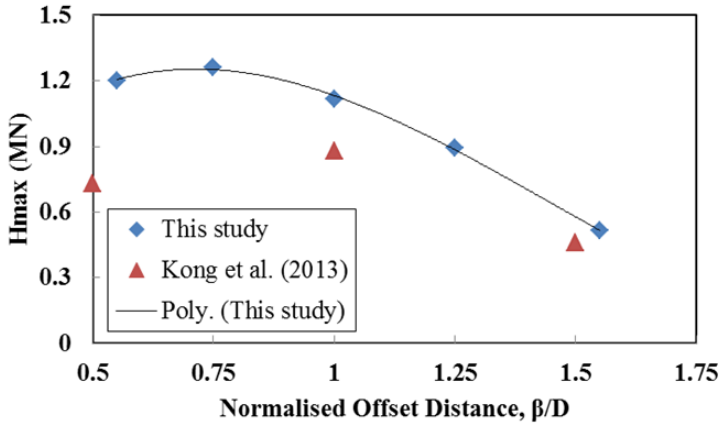

(a)

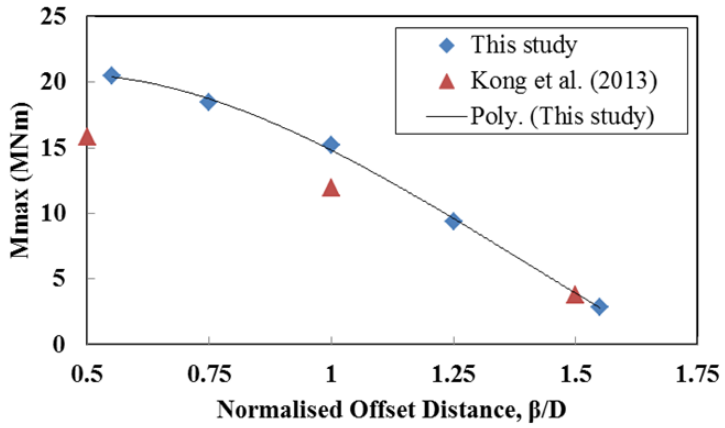

(b)

Figure 8. Effect of the offset distance (β) on the maximum horizontal (H_{max}) and moment (M_{max}) loads

CONCLUSIONS AND FUTURE PLANS

This paper presents a numerical study on the reinstallation process of jack-up platforms using the recently developed 3D LDFE method. The VHM loads and soil failure mechanisms are compared against previously published centrifuge data to validate the reliability of the proposed numerical scheme. An acceptable level of agreement is observed despite the idealisation of the soil material models used in this study. As the normalised parameters of the horizontal and moment loads, the predictions of the load inclination angle and the eccentricity show excellent agreements with the experimental results, which illustrate the capability of the proposed numerical scheme to accurately predict the loads that are directly caused by the footprint geometry. A parametric study is then performed to investigate the effect of the offset distance on the reinstallation processes. The variations in the loads are found to agree with the observed transitions in the soil failure mechanisms. The maximum horizontal and moment loads are plotted against the normalised offset distance to help identify the critical offset distance at which the largest horizontal load (β_{Hmax}=0.75D) and moment (β_{Mmax}=0.55D) are likely to occur.

This study illustrates the capability of the recently developed 3D RITSS method when considering jack-up reinstallation problems. A broad range of sensitivity studies can be conducted to provide a better and more comprehensive understanding to such problems. Moreover, as the 3D RITSS approach adopted in this paper is highly practical with no requirement for intensive user-defined coding while still provides excellent simulation accuracy, it has the potential to be developed for further industrial use in which specific case studies could be performed with real field data.

The following topics are of particular research interest, and some of these are currently being investigated:

Sensitivity studies:

(1) The effect of soil heterogeneity. Variations in the soil strength directly underneath the footprint are considered to be a dominant cause of the extreme loads during the deep penetration stage of the reinstallation processes, particularly in relatively soft clays [5, 17]. The change in the soil strength profile due to the creation of the footprint can be obtained by (a) full numerical installation-retraction simulations or (b) experimental or field measurements, which can then be mapped onto finite element models to facilitate the investigation of the effect of the soil heterogeneity on reinstallation processes.
(2) Footprint size. The size of the footprints dominates the effect of the footprint's geometry on the reinstallation processes. However, depending on the shape of the spudcans, the soil stiffness and the retraction processes used, the depth and diameter of the footprint could vary significantly from case to case. A better understanding of the effect of the footprint's geometry is therefore important.
(3) Structural stiffness. Based on the results from previous experimental studies, such as those in references [8, 10, 11, 13], the lateral and rotational movement of the spudcan produce a significant effect on the load conditions. It is therefore necessary to consider the presence of (a) the lateral stiffness of the leg structure and (b) the stiffness of the leg-platform joints to increase the accuracy of the predictions.

Full-scale reinstallation simulations:

The jack-up structure is simulated in the finite element model to provide a better understanding of the problem being considered. Complex truss-work legs and platform decks are represented with simple beams and plates using equivalent structural stiffnesses. The loads, deformations and movements that occur in the structure during the reinstallation process can therefore be precisely predicted if detailed structural information is available. Together with field data that describes the soil strength profile and the real footprint geometry, accurate and highly customised case studies could be simulated to provide reliable guidelines on the reinstallation process of any jack-up platform at each individual site.

REFERENCES

[1] SNAME., Guidelines for site specific assessment of mobile jack-up units., Technical & Research Bulletin 5-5A, New Jersey: Society of Naval Architects and Marine Engineers. 2008.
[2] Kong VW, Cassidy MJ, Gaudin C, Jack-up reinstallation near a footprint cavity, In: Proceedings of the Seventh International Conference on Physical Modelling in Geotechnics (ICPMG 2010). Zurich, 2010. pp. 1033-1038.
[3] Stewart DP, Finnie IMS, Spudcan-footprint interaction during jack-up workovers, In: The Eleventh International Offshore and Polar Engineering Conference, 2001.
[4] Cassidy MJ, Quah CK, Foo KS, Experimental investigation of the reinstallation of spudcan footings close to existing footprints, Journal of geotechnical and geoenvironmental engineering. 2009:135 (4): 474-486.
[5] Gan CT, Leung CF, Chow YK, A study on spudcan footprint interaction, In: Proceedings of the Second British Geotechnical Association International Conference on Foundations, ICOF, 2008.
[6] Gan CT, Leung CF, Cassidy MJ, Gaudin C, Chow YK, Effect of time on spudcan–footprint interaction in clay, Géotechnique. 2012:62 (5): 401-413.
[7] Gan CT, Centrifuge model study on spudcan-footprint interaction, Ph. D. thesis, National University of Singapore, Singapore, 2009.
[8] Kong VW, Jack-up reinstallation near existing footprints, Ph. D. thesis, University of Western Australia, Australia, 2012.
[9] Kong VW, Cassidy MJ, Gaudin C, Experimental study of effect of geometry on reinstallation of jack-up next to footprint, Canadian Geotechnical Journal. 2013:50 (5): 557-573.
[10] Gaudin C, Cassidy MJ, Donovan T, Grammatikopoulou A, Jardine RJ, Kovacevic N, Potts DM, Hoyle MJR, Hampson KM, Spudcan reinstallation near existing footprints, In: Offshore Site Investigation and Geotechinics, Confronting New Challenges and Sharing Knowledge, 2007.
[11] Gaudin C, Kong V, Cassidy MJ, An Overview of Spudcan Reinstallation Near a Footprint, In: Offshore Technology Conference, 2012.

[12] Dean ER, Serra H, Concepts for mitigation of spudcan-footprint interaction in normally consolidated clay, In: The Fourteenth International Offshore and Polar Engineering Conference, 2004.
[13] Jardine RJ, Kovacevic N, Hoyle MJR, Sidhu HK, Letty A, Assessing The Effects On Jack Up Structures Of Eccentric Installation Over Infilled Craters, In: Offshore Site Investigation and Geotechnics' Diversity and Sustainability'; Proceedings of an International Conference, 2002.
[14] Grammatikopoulou A, Jardine RJ, Kovacevic N, Potts DM, Hoyle MJR, Hampson KM, Potential solutions to the problem of the eccentric installation of Jack-up structures into old footprint craters, In: Offshore Site Investigation and Geotechinics, Confronting New Challenges and Sharing Knowledge, 2007.
[15] Teh KL, Byrne BW, Houlsby GT, Effects of seabed irregularities on loads developed in legs of jack-up units, In: Proceedings of the 1st Jack-up Asia Conference and Exhibition, Singapore, 2006.
[16] Mao D, Zhang M, Yu Y, Duan M, Zhao J, Analysis of spudcan–footprint interaction in a single soil with nonlinear FEM, Petroleum Science. 2015:12 (1): 148-156.
[17] Hartono H, Tho KK, Leung CF, Chow YK, Centrifuge and Numerical Modelling of Reaming as a Mitigation Measure for Spudcan-Footprint Interaction, In: Offshore Technology Conference-Asia, 2014.
[18] Wang D, Bienen B, Nazem M, Tian Y, Zheng J, Pucker T, Randolph MF, Large deformation finite element analyses in geotechnical engineering, Computers and Geotechnics. 2015:65: 104-114.
[19] White DJ, Take WA, Bolton MD, Soil deformation measurement using particle image velocimetry (PIV) and photogrammetry, Géotechnique. 2003:53 (7): 619-631.
[20] Hu Y, Randolph MF, A practical numerical approach for large deformation problems in soil, International Journal for Numerical and Analytical Methods in Geomechanics. 1998:22 (5): 327-350.
[21] Carter JP, Balaam NP, AFENA users manual, Centre for Geotechnical Research, Department of Civil Engineering, University of Sydney, Australia. 1995.
[22] Yu L, Liu J, Kong XJ, Hu Y, Three-dimensional RITSS large displacement finite element method for penetration of foundations into soil, Computers and Geotechnics. 2008:35 (3): 372-382.
[23] Wang D, Hu Y, Randolph MF, Three-dimensional large deformation finite-element analysis of plate anchors in uniform clay, Journal of geotechnical and geoenvironmental engineering. 2009:136 (2): 355-365.
[24] Altair Engineering, Altair HyperMesh 12.0 User's Guide, 2013.
[25] Altair Engineering, Tetra Mesh Optimization, Altair HyperMesh 12.0 User's Guide. 2013: 323-327.
[26] Simulia DS, Abaqus 6.12 documentation, Providence, Rhode Island, US. 2012.
[27] Tian Y, Cassidy MJ, Randolph MF, Wang D, Gaudin C, A simple implementation of RITSS and its application in large deformation analysis, Computers and Geotechnics. 2014:56 (5): 160-167.
[28] Kong VW, Cassidy MJ, Gaudin C, Failure mechanisms of a spudcan penetrating next to an existing footprint, Theoretical and Applied Mechanics Letters. 2014.